Transport through single-wall metallic carbon nanotubes in the cotunneling regime

I. Weymann,[1,2,*] J. Barnaś,[1,3] and S. Krompiewski[3]
[1]*Department of Physics, Adam Mickiewicz University, 61-614 Poznań, Poland*
[2]*Theoretical Physics Department, Institute of Physics, Budapest University of Technology and Economics, H-1521 Budapest, Hungary*
[3]*Institute of Molecular Physics, Polish Academy of Sciences, 60-179 Poznań, Poland*
(Received 11 March 2008; revised manuscript received 22 May 2008; published 14 July 2008)

Using the real-time diagrammatic technique and taking into account both the sequential and cotunneling processes, we analyze the transport properties of single-wall metallic carbon nanotubes coupled to nonmagnetic and ferromagnetic leads in the full range of parameters. In particular, considering the two different shell filling schemes of the nanotubes, we discuss the behavior of the differential conductance, the tunnel magnetoresistance, and the shot noise. We show that in the Coulomb diamonds corresponding to even occupations, the shot noise becomes super-Poissonian due to bunching of fast tunneling processes resulting from the dynamical channel blockade, whereas in the other diamonds the noise is roughly Poissonian, in qualitative agreement with recent experiments. The tunnel magnetoresistance is very sensitive to the number of electrons in the nanotube and exhibits a distinctively different behavior depending on the shell filling sequence of the nanotube.

DOI: 10.1103/PhysRevB.78.035422 PACS number(s): 73.63.Fg, 72.25.Mk, 85.75.−d, 73.23.Hk

I. INTRODUCTION

Transport properties of carbon nanotubes (CNTs) have been a subject of extensive studies for a few years.[1,2] In particular, very recently there has been a growing interest in the shot-noise measurements of CNTs.[3–8] The shot noise provides useful information, not necessarily contained in the current, about the electronic structure, couplings to external leads, and indicates the role of correlations and different types of processes driving the current.[9] In addition, recent experiments on CNTs coupled to ferromagnetic leads have also shown that nanotubes exhibit a considerable tunnel magnetoresistance (TMR) effect.[10–23] The TMR provides information about the spin accumulation on the nanotube and charge states taking part in transport.[23,24]

If the nanotube is weakly coupled to external leads, the current flows through the system due to consecutive tunneling processes. The first-order (sequential) tunneling processes dominate above a certain threshold voltage and are suppressed below this voltage due to the single-electron charging energy and/or finite level separation. On the other hand, current in the blockade regions is mainly mediated by second-order processes (cotunneling).[25] Theoretical considerations of spin-dependent transport properties of single-wall metallic CNTs in the perturbative regime have been so far mainly restricted to the sequential tunneling processes.[22,23] However, because transport in the Coulomb blockade regime is dominated by cotunneling processes, the sequential tunneling approximation may lead to wrong results. Therefore, to get reliable information on the transport properties in the full range of bias and gate voltages, which could be compared with that observed experimentally, one should go beyond the first-order theory. This is the main objective of the present paper.

The considerations are based on the real-time diagrammatic technique, which allows us to take into account the sequential tunneling, cotunneling, and cotunneling-assisted sequential tunneling processes in a fully systematic way. Assuming realistic parameters of the system,[26,27] we calculate the current, differential conductance, TMR, and the shot noise of CNTs. In addition, we also analyze the effect of different shell filling sequences, which can be realized in the single-wall CNTs exhibiting four-electron periodicity[26,27] on transport characteristics. Generally, one can distinguish two different shell filling schemes—in the first scheme the following sequence of the ground states is realized, $S=0,1/2,0,1/2$, where S is the spin of the nanotube, while in the second scheme it is $S=0,1/2,1,1/2$. We show that the effect of different shell filling scenarios is the most visible in the TMR, while the current and shot noise are only slightly affected. This is due to the fact that the TMR directly reflects the magnetic properties of the system and it is thus very sensitive to whether the ground state of the nanotube is a singlet or a triplet. As concerns the shot noise, we show that the corresponding Fano factor F in the Coulomb blockade regions is enhanced above the Schottky value, $F>1$, due to bunching of inelastic cotunneling processes. However, is this enhancement significantly lower than that obtained within the first-order approximation.[23] Contrary, in the transport regions where the sequential contribution to the current is dominant, the shot noise is sub-Poissonian with F slightly above 1/2 and is only weakly modified by the cotunneling processes. Our results for the shot noise are in qualitative agreement with recent experimental data on carbon nanotubes[3] and quantum dots.[28]

The paper is organized as follows. In Sec. II we describe the model of the nanotube and in Sec. III we briefly present the real-time diagrammatic technique used in calculations. Numerical results and their discussion are given in Sec. IV, where we first present the results on CNTs coupled to nonmagnetic leads and then we discuss the effects of spin-dependent tunneling on transport properties. In addition, we also present results for two different shell filling scenarios. Finally, we give the conclusions in Sec. V.

II. MODEL

We consider a single-wall metallic CNT weakly coupled to the two electrodes which can be either nonmagnetic or ferromagnetic. In the latter case the magnetizations of the leads are assumed to be collinear and form either parallel or antiparallel magnetic configuration. The Hamiltonian $\hat{H}$ of the system takes the general form $\hat{H}=\hat{H}_L+\hat{H}_R+\hat{H}_{\rm CNT}+\hat{H}_T$. The first two terms describe noninteracting itinerant electrons in the leads, $\hat{H}_r=\Sigma_{\mathbf{k}\sigma}\varepsilon_{r\mathbf{k}\sigma}c^\dagger_{r\mathbf{k}\sigma}c_{r\mathbf{k}\sigma}$, for the left ($r=L$) and right ($r=R$) leads, with $\varepsilon_{r\mathbf{k}\sigma}$ being the energy of an electron with the wave vector $\mathbf{k}$ and spin σ in the lead r. The third term of $\hat{H}$ describes the single-wall CNT and is given by[29]

$$\hat{H}_{\rm CNT}=\sum_{\mu j\sigma}\varepsilon_{\mu j}n_{\mu j\sigma}+\frac{U}{2}(N-N_0)^2+\delta U\sum_{\mu j}n_{\mu j\uparrow}n_{\mu j\downarrow}+J\sum_{\mu j,\mu' j'}n_{\mu j\uparrow}n_{\mu' j'\downarrow}, \quad (1)$$

where $N=\Sigma_{\mu j\sigma}n_{\mu j\sigma}$, with $n_{\mu j\sigma}=d^\dagger_{\mu j\sigma}d_{\mu j\sigma}$ being the occupation operator for spin σ and jth level in the subband μ ($\mu=1,2$). The energy $\varepsilon_{\mu j}$ of the jth discrete level in the subband μ is given by $\varepsilon_{\mu j}=j\Delta+(\mu-1)\delta$, where Δ is the mean level spacing and δ is the energy mismatch between the two subbands of the nanotube. The charging energy of CNT is described by U, and N_0 is the charge on the nanotube induced by gate voltages. The additional on-level Coulomb energy between two electrons occupying the same orbital level is denoted by δU, whereas J describes the exchange energy between the spin-up and spin-down electrons. The exchange effects described by J play an important role for small diameter nanotubes[30] (up to 2 nm or so), as considered in this paper, whereas for nanotubes of larger diameters these effects become negligible. Finally, the last term of $\hat{H}$, $\hat{H}_T$, takes into account tunneling processes between the nanotube and electrodes, $\hat{H}_T=\Sigma_{r=L,R}\Sigma_{\mathbf{k}}\Sigma_{\mu j\sigma}(t_{rj}c^\dagger_{r\mathbf{k}\sigma}d_{\mu j\sigma}+t^\star_{rj}d^\dagger_{\mu j\sigma}c_{r\mathbf{k}\sigma})$, where t_{rj} denotes the tunnel matrix elements between the lead r and the jth level (assumed to be spin independent also for ferromagnetic leads). Coupling of the jth level to external leads is described by $\Gamma^\sigma_{rj}=2\pi|t_{rj}|^2\rho^\sigma_r$, with ρ^σ_r being the density of states in the lead r for spin σ. The role of ferromagnetic leads is taken into account just via the spin-dependent density of states ρ^σ_r. The coupling parameters can also be expressed as $\Gamma^{+(-)}_{rj}=\Gamma_{rj}(1\pm p_r)$ for the spin-majority (spin-minority) electron bands, with $\Gamma_{rj}=(\Gamma^+_{rj}+\Gamma^-_{rj})/2$ and p_r being the spin polarization of the lead r, $p_r=(\rho^+_r-\rho^-_r)/(\rho^+_r+\rho^-_r)$. For nonmagnetic leads, $\Gamma^+_{rj}=\Gamma^-_{rj}$. In the following we assume $\Gamma_{rj}=\Gamma/2$ for all values of j and r.

III. METHOD

In order to calculate the transport through a single-wall metallic carbon nanotube in the sequential and cotunneling regimes, we employ the real-time diagrammatic technique.[23,31,32] It consists in a systematic expansion of the nanotube (reduced) density matrix and the operators of interest with respect to the coupling strength Γ. The time evolution of the reduced density matrix can be visualized as a sequence of irreducible self-energy blocks, $\mathbf{W}$, on the Keldysh contour. The matrix elements $W_{\chi\chi'}$ of $\mathbf{W}$ describe transitions between the many-body states $|\chi\rangle$ and $|\chi'\rangle$ of the CNT.[23] Then, the Dyson equation constitutes the full propagation of the reduced density matrix, which leads to a kinetic equation for the nanotube occupation probabilities, $(\tilde{\mathbf{W}}\mathbf{p}^{\rm st})_\chi=\Gamma\delta_{\chi\chi_0}$, where $\mathbf{p}^{\rm st}$ is the vector containing probabilities and the matrix $\tilde{\mathbf{W}}$ is given by $\mathbf{W}$ with one arbitrary row χ_0 replaced by $(\Gamma,\ldots,\Gamma)$ due to the normalization condition $\Sigma_\chi p^{\rm st}_\chi=1$. The current flowing through the system can be found from $I=(e/2\hbar){\rm Tr}\{\mathbf{W}^{\rm I}\mathbf{p}^{\rm st}\}$, whereas the zero-frequency current noise, $S=2\int^0_{-\infty}dt(\langle\hat{I}(t)\hat{I}(0)+\hat{I}(0)\hat{I}(t)\rangle-2\langle\hat{I}\rangle^2)$, is given by[32] $S=(e^2/\hbar){\rm Tr}\{[\mathbf{W}^{\rm II}+\mathbf{W}^{\rm I}(\mathbf{P}\mathbf{W}^{\rm I}+\mathbf{p}^{\rm st}\otimes\mathbf{e}^T\partial\mathbf{W}^{\rm I})]\mathbf{p}^{\rm st}\}$. The matrix $\mathbf{W}^{\rm I(II)}$ is the self-energy matrix with one *internal* vertex (two internal vertices), resulting from the expansion of the tunneling Hamiltonian, replaced by the current operator, while the matrices $\partial\mathbf{W}$ and $\partial\mathbf{W}^{\rm I}$ are partial derivatives of $\mathbf{W}$ and $\mathbf{W}^{\rm I}$ with respect to the convergence factor of the Laplace transform.[32] The object $\mathbf{P}$ is calculated from $\tilde{\mathbf{W}}\mathbf{P}=\tilde{\mathbf{1}}(\mathbf{p}^{\rm st}\otimes\mathbf{e}^T-\mathbf{1}-\partial\mathbf{W}\mathbf{p}^{\rm st}\otimes\mathbf{e}^T)$, with $\tilde{\mathbf{1}}$ being the unit vector with row χ_0 set to zero and $\mathbf{e}^T=(1,\ \ldots,1)$.[32] In order to calculate the transport properties order by order in tunneling processes, we expand the self-energy matrices, $\mathbf{W}^{\rm (I,II)}=\mathbf{W}^{\rm (I,II)(1)}+\mathbf{W}^{\rm (I,II)(2)}+\cdots$, and the dot occupations, $\mathbf{p}^{\rm st}=\mathbf{p}^{\rm st(0)}+\mathbf{p}^{\rm st(1)}+\cdots$ and $\mathbf{P}=\mathbf{P}^{(-1)}+\mathbf{P}^{(0)}+\cdots$, respectively. The self-energies can be calculated using the corresponding diagrammatic rules.[24,32,33]

IV. NUMERICAL RESULTS AND DISCUSSION

The shell filling structure of single-wall carbon nanotubes exhibits the four-electron periodicity, which is a consequence of the two spin-degenerate subbands of the nanotube. Furthermore, depending on the intrinsic parameters of the nanotube, its shell filling can generally have two different scenarios.[26,27] The first one is associated with the following sequence of the ground states, $S=0,1/2,0,1/2$, which is realized when $\delta U+J<\delta$. On the other hand, in the second scenario the spin state of the nanotube changes as $S=0,1/2,1,1/2$, which happens for $\delta U+J>\delta$. The difference between these two cases appears in the transport regime where the nanotube is doubly occupied. In the case of first sequence, i.e., for $\delta U+J<\delta$, one orbital level of one of the subbands is fully occupied and the nearest orbital level of the other subband is empty—this is a singlet state. Whereas for $\delta U+J>\delta$, there is a single electron on each level of the two subbands which, due to the exchange interaction J, lead to the formation of a triplet state. In the following, we analyze the behavior of the tunnel magnetoresistance and the shot noise in the linear and nonlinear-response regimes depending on two different shell filling schemes.

A. Shell filling sequence: $S=0,\frac{1}{2},0,\frac{1}{2}$

When $\delta U+J<\delta$, the shell filling of the nanotube is realized in this way that the next orbital levels are being occupied only after the lower lying levels are full, which leads to the sequence of doublet and singlet ground states, S

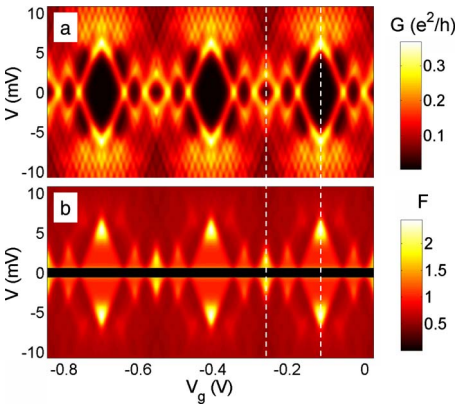

FIG. 1. (Color online) (a) Differential conductance and (b) Fano factor as a function of bias and gate voltages. The parameters are $\Delta=8.4$ meV, $U/\Delta=0.26$, $J/\Delta=0.12$, $\delta U/\Delta=0.04$, $\delta/\Delta=0.27$, $k_BT/\Delta=0.035$, $p_L=p_R=0$, $x=0.14$, and $\Gamma=0.2$ meV.

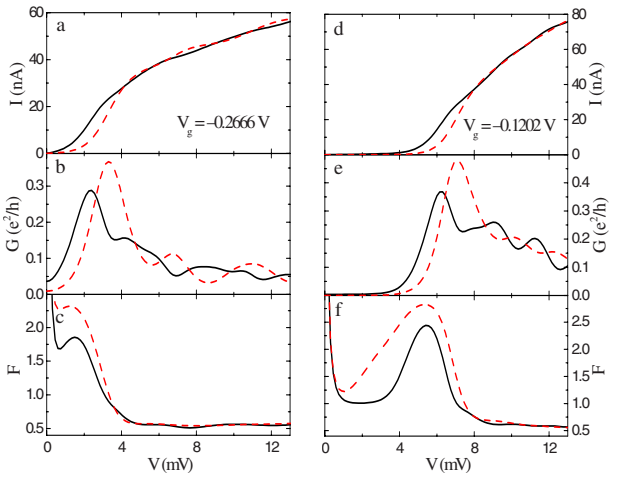

FIG. 2. (Color online) Bias dependence of the current, the differential conductance, and the Fano factor for [(a)–(c)] $V_g=-0.2666$ V and [(d)–(f)] $V_g=-0.1202$ V (see the dashed lines in Fig. 1). The dashed lines show the first-order calculation. The parameters are the same as in Fig. 1.

$=0,1/2,0,1/2$. To model the nanotube in this transport regime, we have taken the experimental parameters derived by Liang *et al.*[26] Furthermore, to clearly elucidate the effect of cotunneling on transport properties, we first present and discuss the behavior of the differential conductance and the Fano factor in the case of CNT coupled to nonmagnetic leads. In this case, for comparison we also show the results obtained when taking into account only the first-order tunneling.

In Fig. 1 we show the density plots of (a) the differential conductance and (b) the Fano factor as a function of the bias and gate voltages. The Fano factor is defined as $F=S/(2e|I|)$ and describes the deviation of S from the Poissonian shot noise given by $S_p=2e|I|$. Since the noise in the small bias regime ($|eV|\leq k_BT$) is dominated by thermal Nyquist-Johnson noise, we excluded this part from considerations and marked it by the black thick line around $V=0$ (the corresponding Fano factor diverges as $V\to 0$). The black diamonds in Fig. 1(a) correspond to blockade regions, where sequential transport is exponentially suppressed and current is dominated by the second-order processes. Furthermore, the four-electron periodicity is clearly visible in the linear conductance, while the additional lines in the differential conductance for voltages larger than the threshold for sequential tunneling are due to excited states participating in transport.

To see clearly the contribution from cotunneling processes we show in Fig. 2 the (a) current, (b) conductance, and (c) Fano factor for two different values of the gate voltage, corresponding to vertical cross sections in Fig. 1 through small and large Coulomb diamonds (see the dashed lines in Fig. 1). Additionally, in Fig. 2 we also show the corresponding quantities calculated in the first order (dashed lines). It is evident that the cotunneling processes modify the current mainly in the blockade regime and also close to resonance (blockade threshold), leading to renormalization of the nanotube levels. This makes the conductance peak shifted toward smaller voltages. In addition, due to the renormalization of the nanotube levels and smearing out of the Coulomb steps caused by cotunneling, in some range of the bias voltage the total current may be smaller than the sequential one [see Figs. 2(a) and 2(d)]. As regard to the shot noise, cotunneling processes have a significant impact on the Fano factor, particularly in the blockade regions corresponding to even occupations, where the shot noise is super-Poissonian. The corresponding Fano factor is then larger than unity but significantly reduced in comparison to that calculated in the first-order approximation.

Consider first the limit of sequential (first-order) tunneling processes. The sequential tunneling starts when the bias approaches the threshold voltage. Owing to the Fermi distribution, sequential processes start before the zero-temperature threshold is reached. When the highest populated level is doubly occupied, tunneling from the source to the drain electrode may leave the nanotube either in the initial or in an excited state. When the CNT is left in the initial state, the next tunneling process goes with the same probability as the first one. When, however, the CNT is left in an excited state, the thermal (dynamical) blockade is lifted and the subsequent tunneling processes are faster. This leads to bunching of fast tunneling processes, which leads to the super-Poissonian shot noise.[34–38]

The cotunneling processes, both single-barrier and two-barrier ones, are not blocked. Generally, there are elastic and inelastic ones, which occur with different probabilities. However, the asymmetry between the fast and slow ones is reduced in comparison with the first order, which leads to a smaller Fano factor when the second-order processes are included. Apart from this, the inelastic cotunneling processes also lift the dynamical blockade of the sequential processes.

It is easy to note that the above scenario does not hold when the highest level is singly occupied. In such a case first-order tunneling processes are of comparable velocity and therefore the Fano factor is only slightly above unity. This applies also to cotunneling processes. Thus, depending on the ground state of the nanotube which can be changed by the gate voltage, we either find a considerable enhancement of the Fano factor (super-Poissonian shot noise) or the Fano

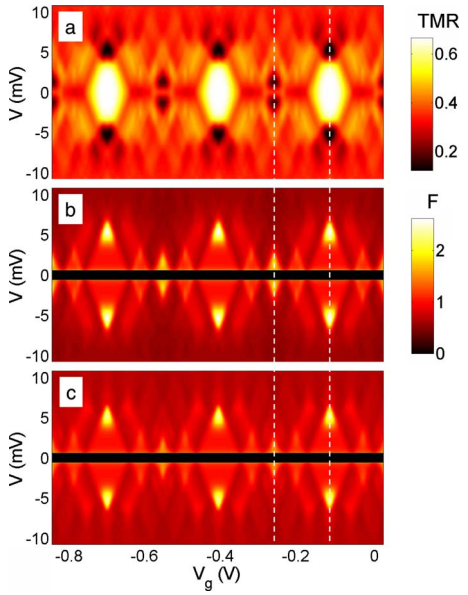

FIG. 3. (Color online) (a) Tunnel magnetoresistance and Fano factor in the (b) parallel and (c) antiparallel configurations as a function of bias and gate voltages. The parameters are as in Fig. 1 with $p_L=p_R=0.5$.

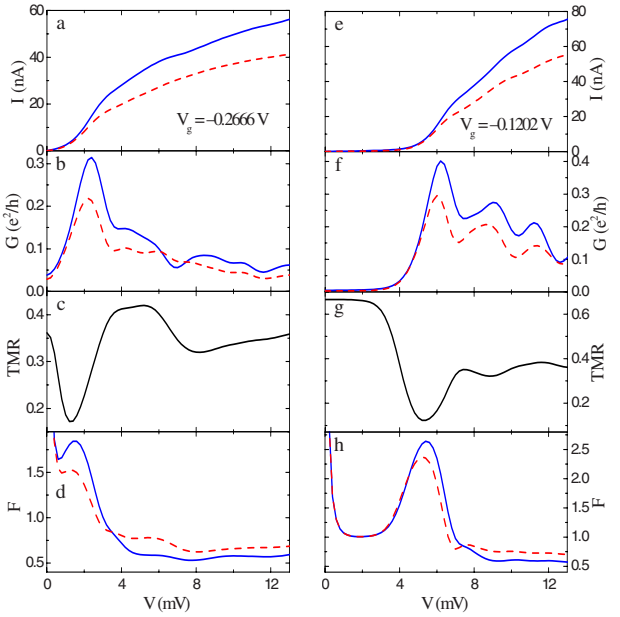

FIG. 4. (Color online) Bias dependence of the current, the differential conductance, the TMR, and the Fano factor in the parallel (solid line) and antiparallel (dashed line) configurations for [(a)-(d)] $V_g=-0.2666$ V and [(e)-(h)] $V_g=-0.1202$ V (see the dashed lines in Fig. 3). The parameters are the same as in Fig. 3.

factor is approximately equal to unity (Poissonian shot noise). This observation, as far as the main trends are concerned, is in agreement with recent experiments carried out by Onac *et al.*[3]—although in view of the limitations of the present theory (perturbation approach, wide bandwidth approximation, symmetric barriers, etc.), the provided insight is basically qualitative in nature. Finally, it is noteworthy that outside the blockade regions the shot noise becomes sub-Poissonian and the corrections due to cotunneling processes are much smaller than in the blockade regime, although still noticeable.

Consider now the numerical results on CNTs contacted to ferromagnetic leads (see Fig. 3). The tunnel magnetoresistance [Fig. 3(a)] exhibits a distinctively different behavior depending on the number of electrons on the nanotube. In the linear-response regime, between the two consecutive four-electron sequences, the TMR is given by the Julliere's formula, $\mathrm{TMR}=2p_Lp_R/(1-p_Lp_R)$,[39] whereas in the other transport regimes it is suppressed below the Julliere's value.[39] This is a completely different feature as compared to the sequential tunneling results where the linear-response TMR is constant and given by $\mathrm{TMR}_{\mathrm{seq}}=p_Lp_R/(1-p_Lp_R)$, irrespective of the gate voltage.[22,23]

In Figs. 3(b) and 3(c) we show the density plots of the Fano factors in both parallel and antiparallel magnetic configurations. The general features of the Fano factors are similar to those in the limit of nonmagnetic leads, except for the fact that now there is an additional contribution to the shot noise coming from the difference between the two spin channels for transport. Because the resultant coupling of the nanotube to ferromagnetic leads in the parallel configuration is larger than in the antiparallel one, the fluctuations of the current are enhanced in the parallel configuration as compared to the antiparallel one. This leads to the corresponding difference in the Fano factors [see Figs. 3(b) and 3(c)], which is especially visible in the Coulomb blockade regime. We also note that although the magnitudes of the Fano factors in both magnetic configurations are different, their general behavior is qualitatively similar.

The bias dependence of the current, conductance, TMR, and the Fano factor is shown in Fig. 4 for two different values of the gate voltage and for both the parallel and antiparallel magnetic configurations. All the quantities are calculated taking into account both the sequential and cotunneling processes, and we do not distinguish between the first- and second-order contributions. As in the case of nonmagnetic leads, the second-order processes significantly modify the TMR and Fano factor in the blockade regions and only slightly outside these regions. An interesting feature is a drop of the TMR at the onset for sequential tunneling [see Figs. 4(c) and 4(g)], which is present when the ground state of the nanotube is a singlet. This is due to the interplay of the inelastic cotunneling processes which flip the spin of electrons occupying the nanotube and the sequential tunneling which is generally incoherent. On the other hand, when the ground state of the nanotube is a doublet, the TMR does not drop with approaching the threshold [see Fig. 3(a)], which is due to a nonequilibrium spin accumulation induced in the nanotube. The spin accumulation tends to increase the TMR and, thus, reduces the role of the above-mentioned processes responsible for TMR drop in the case of ground state $S=0$.

B. Shell filling sequence: $S=0,\frac{1}{2},1,\frac{1}{2}$

The intrinsic parameters of the nanotube depend mainly on their size and coupling to external leads.[26,27] In particular,

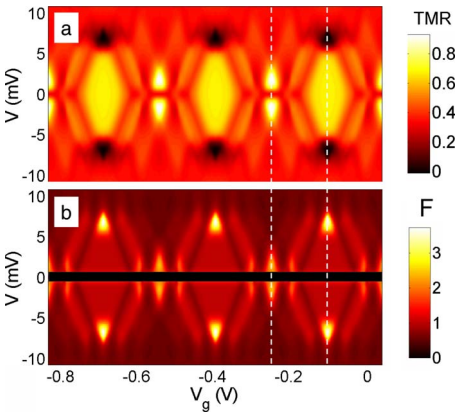

FIG. 5. (Color online) (a) Tunnel magnetoresistance and (b) Fano factor in the parallel configuration as a function of bias and gate voltages. The parameters are the same as in Fig. 3 with $\delta/\Delta = 0.1$.

the quality of the coupling between the leads and nanotube contributes to the energy mismatch δ between the two CNT's subbands. In the case when $\delta U + J > \delta$, the sequence of the ground states is changed as compared to the case of $\delta U + J < \delta$. Now, in the charge state with two electrons in the nanotube, each electron occupies one orbital level of the two subbands. This, together with a finite J, leads to the formation of a triplet state in the nanotube. Thus, the shell filling sequence becomes $S = 0, 1/2, 1, 1/2$.

In Fig. 5 we show the TMR and the Fano factor in the parallel configuration as a function of the bias and gate voltages. The Fano factor in the antiparallel configuration is generally smaller than that in the parallel one, but its behavior is qualitatively similar, therefore we only show F in the parallel configuration—it is displayed in Fig. 5(b). Furthermore, it can be seen that the general behavior of the Fano factor is similar to that in the case of $\delta U + J < \delta$ [see Figs. 1(b) and 3(b)]. Now, the Fano factor becomes super-Poissonian when the ground state of the nanotube is either a singlet or a triplet. This fact is rather intuitive as the dependence of the shot noise on the bias and gate voltages is rather conditioned by the charge states taking part in transport than by the magnetic state of the system. The information about the spin state of the nanotube is mainly contained in the TMR, which for $\delta U + J > \delta$ becomes considerably modified, especially in the transport regime where the ground state is a triplet [see Fig. 5(a)].

The bias voltage dependence of the current, differential conductance, Fano factor in the parallel and antiparallel configurations, as well as of the TMR is shown in Fig. 6. One can now clearly see that general features of transport characteristics calculated for $V_g = -0.2544$ V, i.e., when the ground state of the nanotube is a singlet, are similar to those shown in Figs. 4(a)–4(d). The only differences are the enhancement of the Fano factor at resonance [see Fig. 6(f)] and the drop of the TMR at the onset of sequential tunneling where now TMR becomes slightly negative [see Fig. 6(g)]. On the other hand, when the ground state of the nanotube is a triplet ($V_g = -0.108$ V), the transport characteristics become even more modified [see Figs. 4(e)–4(g) and 6(e)–6(g)]. The main difference is visible in the behavior of the TMR which for $\delta U + J > \delta$ is increased above the Julliere's value.[39] This is associated with the nonequilibrium spin accumulation in triplet states, which tends to enhance the difference between the two magnetic configurations of the system. Furthermore, it is also due to a finite exchange interaction J because of which only particular components of triplet take part in transport. In this way, the exchange interaction plays a role similar to an external magnetic field. As already shown in the case of quantum dots, the TMR may be enhanced above the Julliere's value[39] when only particular spin states of the dot participate in transport.[38]

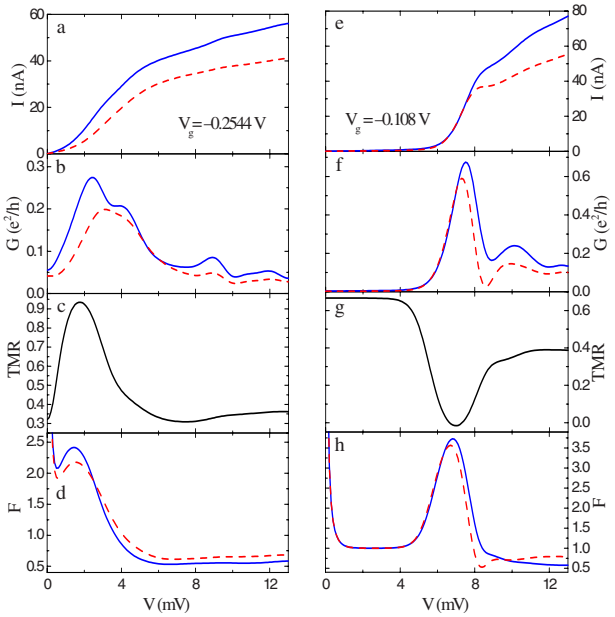

FIG. 6. (Color online) Bias dependence of the current, the differential conductance, the TMR, and the Fano factor in the parallel (solid line) and antiparallel (dashed line) configuration for [(a)-(d)] $V_g = -0.2544$ V and [(e)-(h)] $V_g = -0.108$ V, corresponding to the dashed lines in Fig. 5. The parameters are the same as in Fig. 5.

V. CONCLUDING REMARKS

In conclusion, we have calculated transport characteristics, including shot noise and tunnel magnetoresistance, of CNTs weakly coupled to magnetic and nonmagnetic leads. We have also analyzed the effects of two different shell filling scenarios, which can be realized in single-wall metallic CNTs on transport characteristics. In particular, we have shown that the second-order contributions are crucial in the blockade regions. Depending on the ground state of the nanotube, the shot noise is either super-Poissonian due to the bunching of fast tunneling processes or approximately given by the Poisson value, in qualitative agreement with recent experiments.[3] On the other hand, in the regions dominated by sequential transport processes the shot noise is sub-Poissonian with the corresponding Fano factor roughly equal

to 1/2. Furthermore, we have also shown that the linear TMR exhibits a strong dependence on the gate voltage, being equal to the Julliere's TMR (Ref. 39) in transport regime between the two consecutive four-electron fillings and suppressed below that value in the other transport regimes. In addition, when the ground state of the nanotube is a triplet, the TMR in the nonlinear-response regime at the onset for sequential tunneling becomes enhanced above the Julliere's value,[39] which is due to nonequilibrium spin accumulation in triplet states and finite exchange interaction J.

ACKNOWLEDGMENTS

This work was supported by the EU grant CARDEQ under Contract No. IST-021285–2 and, as part of the European Science Foundation EUROCORES Programme SPINTRA under Contract No. ERAS-CT-2003–980409, by funds from the Ministry of Science and Higher Education as a research project in years 2006–2009. I.W. also acknowledges support from the Foundation for Polish Science and the hospitality of BUTE.

*weymann@amu.edu.pl

[1] R. Saito, M. S. Dresselhaus, and G. Dresselhaus, *Physical Properties of Carbon Nanotubes* (Imperial College, London, UK, 1998).
[2] M. P. Anantram and F. Leonard, Rep. Prog. Phys. **69**, 507 (2006).
[3] E. Onac, F. Balestro, B. Trauzettel, C. F. J. Lodewijk, and L. P. Kouwenhoven, Phys. Rev. Lett. **96**, 026803 (2006).
[4] F. Wu, T. Tsuneta, R. Tarkiainen, D. Gunnarsson, T.-H. Wang, and P. J. Hakonen, Phys. Rev. B **75**, 125419 (2007).
[5] F. Wu, P. Queipo, T. Tsuneta, T. H. Wang, E. Kauppinen, and P. J. Hakonen, Phys. Rev. Lett. **99**, 156803 (2007).
[6] T. Tsuneta, P. Virtanen, F. Wu, T. Wang, T. T. Heikkilä, and P. J. Hakonen, arXiv:0706.2658 (unpublished).
[7] L. G. Herrmann, T. Delattre, P. Morfin, J.-M. Berroir, B. Placais, D. C. Glattli, and T. Kontos, Phys. Rev. Lett. **99**, 156804 (2007).
[8] N. Y. Kim, P. Recher, W. D. Oliver, Y. Yamamoto, J. Kong, and H. Dai, Phys. Rev. Lett. **99**, 036802 (2007).
[9] Ya. M. Blanter and M. Büttiker, Phys. Rep. **336**, 1 (2000).
[10] K. Tsukagoshi, B. W. Alphenaar, and H. Ago, Nature (London) **401**, 572 (1999).
[11] B. Zhao, I. Mönch, H. Vinzelberg, T. Mühl, and C. M. Schneider, Appl. Phys. Lett. **80**, 3144 (2002).
[12] Jae-Ryoung Kim, Hye Mi So, Ju-Jin Kim, and Jinhee Kim, Phys. Rev. B **66**, 233401 (2002).
[13] S. Sahoo, T. Kontos, J. Furer, C. Hoffmann, M. Gräber, A. Cottet, and C. Schönenberger, Nat. Phys. **1**, 99 (2005).
[14] A. Jensen, J. R. Hauptmann, J. Nygard, and P. E. Lindelof, Phys. Rev. B **72**, 035419 (2005).
[15] H. T. Man, I. J. W. Wever, and A. F. Morpurgo, Phys. Rev. B **73**, 241401(R) (2006).
[16] L. W. Liu, J. H. Fang, L. Lu, H. F. Yang, A. Z. Jin, and C. Z. Gu, Phys. Rev. B **74**, 245429 (2006).
[17] B. Nagabhirava, T. Bansal, G. U. Sumanasekera, B. W. Alphenaara, and L. Liu, Appl. Phys. Lett. **88**, 023503 (2006).
[18] S. Krompiewski, Phys. Status Solidi B **242**, 226 (2005); Semicond. Sci. Technol. **21**, S96 (2006).
[19] A. Cottet and M.-S. Choi, Phys. Rev. B **74**, 235316 (2006).
[20] A. Cottet, T. Kontos, S. Sahoo, H. T. Man, M.-S. Choi, W. Belzig, C. Bruder, A. F. Morpurgo, and C. Schönenberger, Semicond. Sci. Technol. **21**, S78 (2006).
[21] C. Schönenberger, Semicond. Sci. Technol. **21**, S1 (2006).
[22] S. Koller, L. Mayrhofer, and M. Grifoni, New J. Phys. **9**, 348 (2007).
[23] I. Weymann, J. Barnaś, and S. Krompiewski, Phys. Rev. B **76**, 155408 (2007).
[24] I. Weymann, J. König, J. Martinek, J. Barnaś, and G. Schön, Phys. Rev. B **72**, 115334 (2005).
[25] D. V. Averin and Yu. V. Nazarov, Phys. Rev. Lett. **65**, 2446 (1990); K. Kang and B. I. Min, Phys. Rev. B **55**, 15412 (1997).
[26] W. Liang, M. Bockrath, and H. Park, Phys. Rev. Lett. **88**, 126801 (2002).
[27] S. Sapmaz, P. Jarillo-Herrero, J. Kong, C. Dekker, L. P. Kouwenhoven, and H. S. J. van der Zant, Phys. Rev. B **71**, 153402 (2005).
[28] Y. Zhang, L. DiCarlo, D. T. McClure, M. Yamamoto, S. Tarucha, C. M. Marcus, M. P. Hanson, and A. C. Gossard, Phys. Rev. Lett. **99**, 036603 (2007).
[29] Y. Oreg, K. Byczuk, and B. I. Halperin, Phys. Rev. Lett. **85**, 365 (2000).
[30] L. Mayrhofer and M. Grifoni, Phys. Rev. B **74**, 121403(R) (2006).
[31] H. Schoeller and G. Schön, Phys. Rev. B **50**, 18436 (1994); J. König, J. Schmid, H. Schoeller, and G. Schön, *ibid.* **54**, 16820 (1996).
[32] A. Thielmann, M. H. Hettler, J. König, and G. Schön, Phys. Rev. Lett. **95**, 146806 (2005).
[33] I. Weymann, arXiv:0806.4603, Phys. Rev. B (to be published).
[34] B. R. Bułka, Phys. Rev. B **62**, 1186 (2000).
[35] E. V. Sukhorukov, G. Burkard, and D. Loss, Phys. Rev. B **63**, 125315 (2001).
[36] A. Cottet, W. Belzig, and C. Bruder, Phys. Rev. B **70**, 115315 (2004); Phys. Rev. Lett. **92**, 206801 (2004).
[37] W. Belzig, Phys. Rev. B **71**, 161301(R) (2005).
[38] I. Weymann and J. Barnaś, J. Phys.: Condens. Matter **19**, 096208 (2007); Phys. Rev. B **77**, 075305 (2008).
[39] M. Julliere, Phys. Lett. **54A**, 225 (1975).